Crystal Structure of the α-Form of Poly(L-lactide)

C. Alemán, B. Lotz,† and J. Puiggali*

Departament d'Enginyeria Química, ETS d'Enginyeria Industrial, Universitat Politècnica de Catalunya, Diagonal 647, Barcelona E-08028, Spain

Received September 21, 2000; Revised Manuscript Received April 28, 2001

ABSTRACT: Study on the molecular packing of the α-form of poly(L-lactide) has been attempted taking into account packing energy calculations, refinement against new electron diffraction data, and Monte Carlo simulations. Packing energy has been evaluated for a fixed 10_7 conformation and an antiparallel arrangement of molecular chains. The energetically allowed space seems to be quite restricted, but with several minima of similar energy. One of them corresponds to a $P2_12_12_1$ space group and agrees with the structure refined against diffraction data. Moreover, Monte Carlo simulations show a spontaneous evolution toward the refined model when parameters that define the packing, such as chain axis shift and setting orientation angles, are relaxed. On the other hand, the proposed packing shows asymmetric interactions that may lead to a molecular distortion.

Introduction

Poly(L-lactide) ($-[CH_2CH(CH_3)COO]_n-$) is a biodegradable and biocompatible crystalline polymer[1−3] with potential applications as a suture in microsurgery, since it could be processed into high-strength fibers.[4] Depending on spinning and drawing conditions,[5] two crystals modifications (α- and *β*-forms) are found. The latter is observed at high draw ratio and drawing temperature and was reported for the first time by Eling and co-workers.[2] Its conformation corresponds to a 3-fold helix,[5] and its packing has recently been interpreted[6] on the basis of a *frustrated structure*, which has a trigonal cell with three chains. A new crystal modification, the *γ* form, has recently been obtained by epitaxial crystallizations on hexamethylbenzene.[7] In this case, two 3-fold helices are arranged in an antiparallel disposition in the orthorhombic unit cell.

The conformation of the most stable α-form was determined from conformational analysis by De Santis and Kovacs[8] and corresponds to a 10_7 helix. However, X-ray fiber diffraction patterns display some extra meridional reflections that indicate some distortion from the pure 10_7 conformation. It has been suggested[5] that the interchain contacts between methyl groups force this distortion, in a way similar to the α-helix conformation of poly(L-alanine),[9] which is the polypeptide analogous of poly(L-lactide).

The PLLA α-form is obtained by crystallization from dilute solutions (*p*-xylene at 90 °C[10] or acetonitrile at 25 °C[11]). The single crystals show a lozenge habit and a characteristic *hk*0 electron diffraction pattern, which features will be discussed below. Unit cell parameters of the α-form reported by different authors[5,8,11,12] are essentially similar, although some minor differences can be found. Thus, they correspond to an orthorhombic lattice with dimensions varying in the intervals a = 10.78−10.50 Å, b = 6.45−6.04 Å, and c (chain axis) = 27.8−28.8 Å. However, neither the packing mode nor the type of distortion of the 10_7 helices has been established. The main purpose of this work is to progress in the elucidation of this structure taking into account new 0*kl* electron diffraction data from epitaxial crystallization,[7] packing energy considerations, and modeling simulations. Furthermore, the proposed packing mode has been analyzed in detail using Monte Carlo (MC) simulations.

Methods

Energy Calculations. Energy calculations were performed with the PCSP (Prediction of the Crystal Structure of Polymers) computer program.[13] This program generates the atomic coordinates of a polymer in a given crystal lattice, the parameters of which are known from diffraction analysis, and evaluates the energy of the resulting structure. Specifically, the program explores the relative stability of the structures when chain axis shift and setting angles of the molecules are varied.

Calculations made by PCSP include the energy contributions of van der Waals and electrostatic interactions between nonbonded atoms by applying Lennard-Jones 6−12 and Coulombic expressions, respectively. The van der Waals parameters are taken from the anisotropic parametrization of the AMBER force field; i.e., the CH_3 group is considered as a single sphere whereas the remaining atoms are explicitly included.[14] The partial atomic charges were derived using a methodology previously developed.[15] The lattice dimensions chosen for the PCSP calculations are those given by Hoogsteen et al.:[5] a = 10.60 Å, b = 6.10 Å, and c = 28.8 Å. Their atomic coordinates were also used to build the conformation of the repeat unit of poly(L-lactide) (Figure 1) and then the 10_7 helix (dihedral angles are φ = −64.8°, ψ = 148.9°, and ω = 179.5°). Periodic boundary conditions are applied in the *a*-, *b*-, and *c*-axes. A cutoff limit of 10 Å is imposed: within this limit, all atoms of one residue interacting with other residues are included.

Modeling Simulations. For structural refinement we take into account both the *hk*0 and 0*kl* electron diffraction patterns of poly(L-lactide) in its α form (Figure 2). These patterns were obtained[6] from solution-grown single crystals and thin films epitaxially crystallized on hexamethylbenzene, respectively. Electron diffraction patterns were simulated with the appropriate

† Permanent address: Institut Charles Sadron (CNRS-ULP), 6 rue Boussingault, 67083 Strasbourg, France.
* Corresponding author. E-mail: puiggali@eq.upc.es.

10.1021/ma001630o CCC: $20.00
Published on Web 06/09/2001

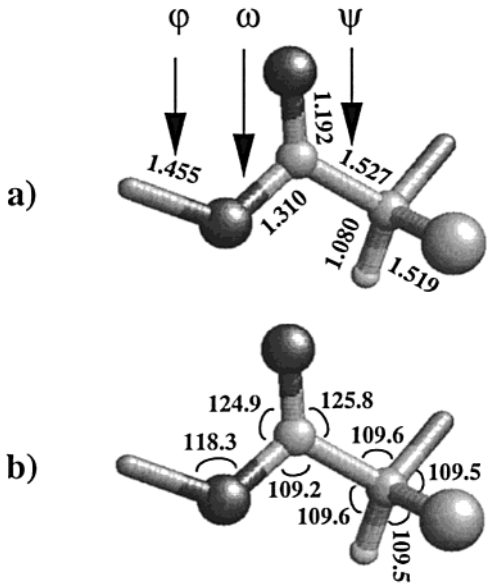

Figure 1. Bond lengths (Å) (a) and angles (deg) (b) of poly(L-lactide) calculated using the Cartesian coordinates reported by Hoogsteen et al.[5] The torsional angles φ, ψ, and ω are indicated.

packages of the CERIUS[2] program.[16] Different space groups, setting angle orientations, and relative shift of molecules in the unit cell were considered. The packing arrangements provided by PCSP calculations were also taken into account. Molecular conformation was not optimized during the refining process.

Monte Carlo Simulations. MC simulations were performed using the parallelized version of the MCDP[17] (Monte Carlo simulations of Dense Polymers) computer program, which was explicitly designed to simulate the crystal structure of synthetic polymers. The atomistic model consisted of eight independent chains, which were packed in an orthorhombic box with the helix axes oriented parallel to the *c*-axis at the positions indicated in Figure 3. Periodic boundary conditions and the minimum-image convention were applied to all simulations. Nonbonded interactions were again neglected beyond 10 Å. The *x*- and *y*-edges of the simulation box were doubled with respect to the crystallographic unit cell (Figure 3) in order to avoid interactions between any one chain and its image.

The model used in the MC simulations assumes fixed bond lengths and bond angles (Figure 1). Therefore, the degrees of freedom in simulations of *NVT* type, i.e., without varying the size of the box, are the torsional angles (φ, ψ, and ω), the setting angles, and the displacement of the helices along the *c*-axis. In these simulations the box edges were defined as displayed in Figure 3. On the other hand, in *NPT* type simulations (P = 1 atm), conformational and molecular displacements along the three axes were combined with volume changes; i.e., the lengths of the edges of the simulation box were also considered as degrees of freedom. All the movements were performed using the Metropolis algorithm,[18] and the left-handed 10_7 helix symmetry, i.e., 3.333 residues per turn, was kept fixed in all the simulations.

The potential functions and force-field parameters used for van der Waals and electrostatic energies are the same as in PCSP calculations. A three-term Fourier series expansion was used to compute the torsional energy, where the torsional angles are calculated between all pairs of atoms that have a 1−4 interaction. Torsional parameters were taken from AMBER libraries.[14]

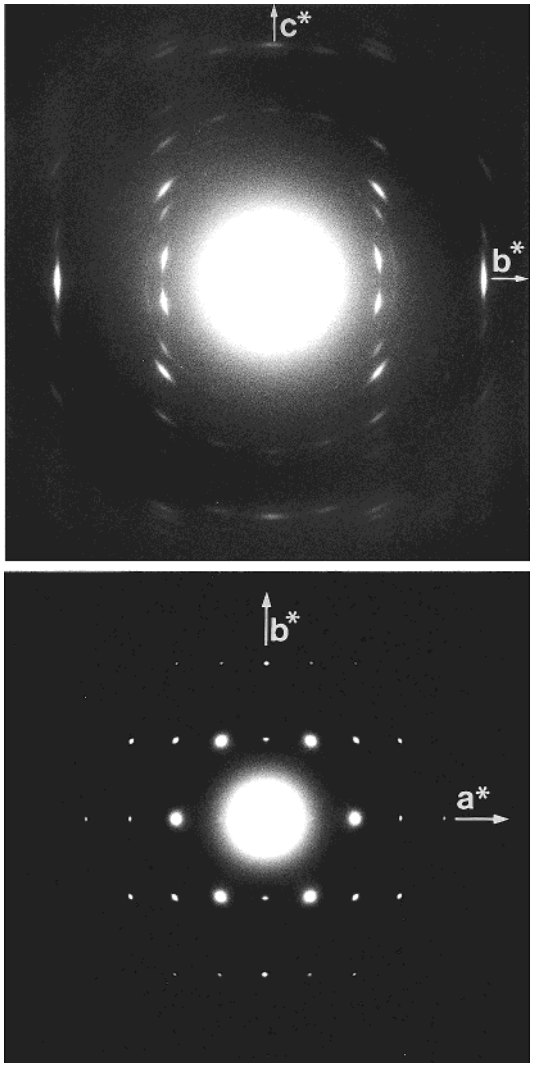

Figure 2. (a) 0*kl* electron diffraction pattern of an epitaxially crystallized film of poly(L-lactide) on a single crystal of hexamethylbenzene. A slight tilt about the *b* axis is apparent through the presence, on the upper layer lines, of reflections from parallel reciprocal planes, i.e., 1*kl*. (b) *hk*0 electron diffraction pattern of a single crystal of poly(L-lactide) grown by slow cooling from 90 °C of a solution in *p*-xylene.

Results and Discussion

PCSP Calculations. A unit cell with two antiparallel helices (Figure 4a) was considered, since it agrees with experimental information (see next section). The system was defined by using only three variables: (a) the angle (τ) measured between the *a* axis and the vector linking the *ab* projections of the helix center and a representative C^α atom of the first chain; (b) the angle (θ) measured in a similar way by using a C^α atom of the second chain; and (c) the *c* chain shift (Δz) measured as the difference ($z_1 - z_2$) between the fractional coordinates of the chosen C^α. Thus, the angles τ and θ define the setting orientation of the two helices and Δz is their relative shift.

In a first step, a packing energy study was carried out in order to determine the most favorable setting angle of the parent chain. For this purpose three chains were arranged in parallel at a distance of 6.10 Å, i.e.,

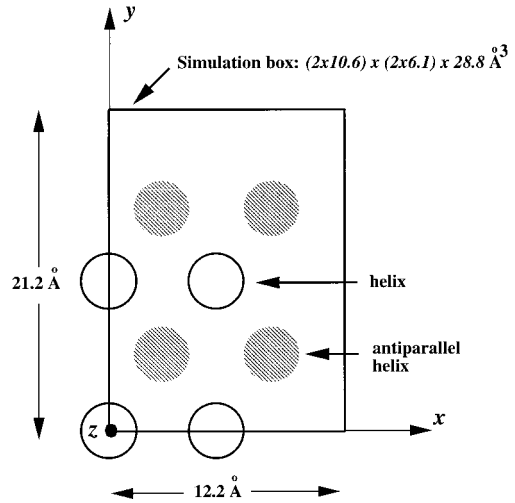

Figure 3. Schematic representation of the coordinate system used in the Monte Carlo simulation. The view is along the helix axis (*c*-axis). Only the eight parent-chain helices are represented. Open and dashed circles represent positions of parallel and antiparallel chains, respectively.

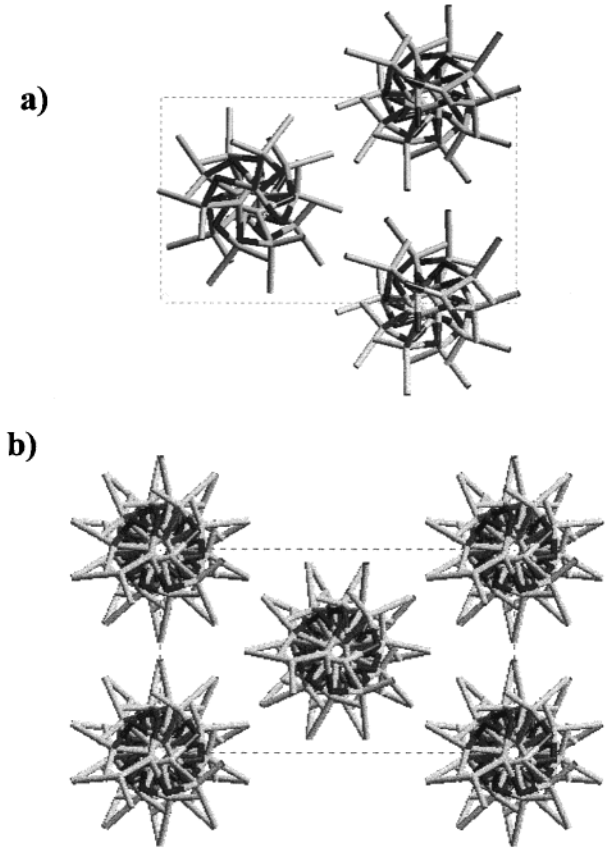

Figure 4. *ab* projections of the optimized packing of poly(L-lactide) in the $P2_12_12_1$ (a) and $P222_1$ (b) space groups.

the length of the *b*-axis.[5] The setting angle τ was varied from 0° to 360° in steps of 10° and the energy per residue evaluated. Figure 5a plots the energy as a function of the setting angle τ. The most favorable arrangement corresponds to $\tau = 150°$ (or $-30°$), which was used in all the successive calculations, i.e., in both PCSP and MC simulations, to fix the orientation of the parent chain in the unit cell. Note that the energy profile is symmetrical from $-180°$ to 0° and from 0° to 180° due to the symmetric environment of the central chain.

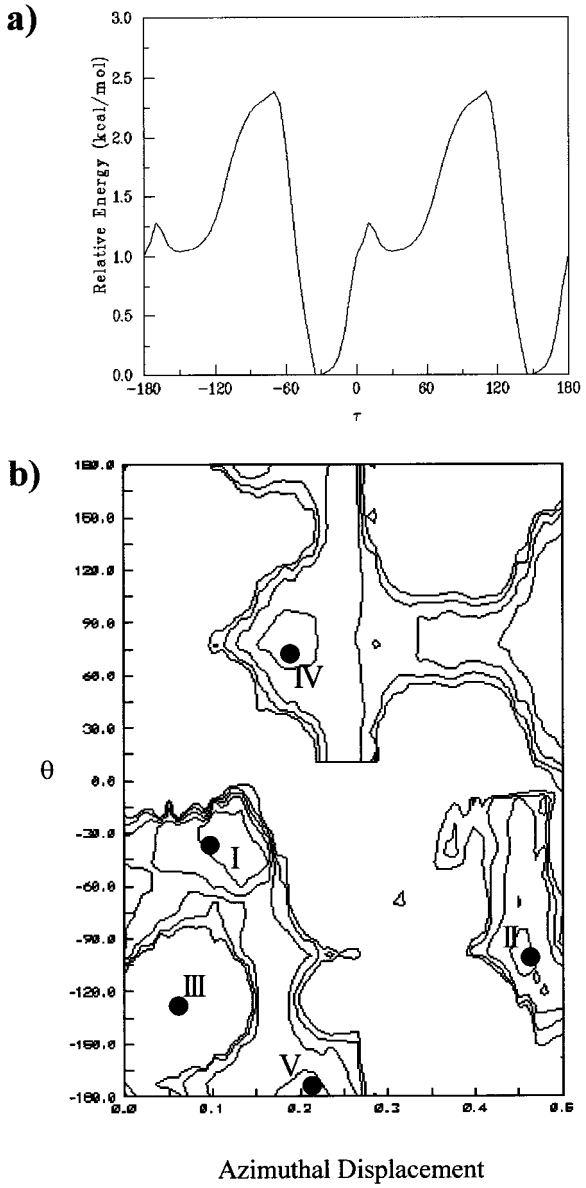

Figure 5. (a) Plot of the energy for three isolated parallel chains as a function of the setting angle τ. (b) Energy map computed for poly(L-lactide) considering a packing of antiparallel molecular chains. The setting angles and the energy are expressed in degrees and kcal/mol, respectively. The *c* axis shift is expressed in fractional coordinates. Contour lines are drawn at a 1 kcal/mol interval.

Next, the most favorable arrangement of the poly(L-lactide) chains within the unit cell was determined by computing the potential energy surface $E = E(\Delta z, \theta, \tau = 150°)$. No symmetry constraint was imposed since the PCSP program evaluates the energy with respect to a given residue. Thus, the environment of such a residue is different for every position, even though some positions may be equivalent from a crystallographic point of view; i.e., all the positions within the chain are distinguishable when the energy is evaluated with respect to a given residue. Initially, the variables Δz and θ were systematically varied from 0 to 1 and from 0° to 360°, respectively, using grid steps of 0.10 and 20°. Results provided a rough picture of the potential energy surface, which was found to be nonsymmetric with respect to $\Delta z = 0.5$. These energy differences are due to the 10_7 helix symmetry: the packing environment, which is calculated with respect to a given residue, is

Table 1. Minimum-Energy Packing Modes Obtained from PCSP Calculations and MC Simulations of *NPT* Type

	PCSP			MC			
minimum	ΔE^a	θ^b	Δz^c	ΔE^a	τ^b	θ^b	Δz^c
I	0.0	−39	0.11	0.0	149	−30	0.15
II	0.1	−99	0.47	0.5	155	−104	0.41
III	0.1	−127	0.07	−0.1	159	−144	0.00
IV	0.3	73	0.19	1.4	−140	88	0.24
V	0.3	−178	0.22	−0.4	132	180	0.25

[a] Relative energies (in kcal/mol of residue). [b] Setting angles (in deg). [c] Chain axis shift (in fractional coordinates).

different for the 10 residues included in the axial repeat length, and consequently the intermolecular interactions change with θ and Δz. In all cases, minimum-energy packing modes for $\Delta z < 0.5$ were at least 4 kcal/mol more stable than for $\Delta z > 0.5$. Accordingly, the bidimensional energy map was recomputed within this range but using finer grid steps, i.e., 0.02 and 10° for Δz and θ, respectively. The resulting potential energy surface $E = E(\Delta z, \theta, \tau = 150°)$ is displayed in Figure 5b. The contour lines correspond to1 kcal/mol intervals.

The energetically allowed space is quite restricted. θ values ranging from 0° to 180° for $\Delta z < 0.15$ and from −180° to 0° for $0.25 < \Delta z < 0.40$ are forbidden due to steric conflicts. Furthermore, for regions with lower energy, the energy surface is rather flat in the θ reaction coordinate. Five low-energy arrangements can be seen in Figure 5b (indicated by black dots). Table 1 lists their Δz and θ coordinates as well as their relative energies. Note that energy are below 0.5 kcal/mol and not therefore very discriminative. Accordingly, the five minima were further investigated and further compared to electron diffraction data and Monte Carlo simulations. However, minimum I in Figure 5b and Table 1 corresponds to an arrangement strikingly close to the $P2_12_12_1$ space group. This feature is clearer when the position of the second chain is defined by a residue different from that used in the energy calculations (from now on, we use primed symbols for this new denomination). Thus, the second chain is defined by $\theta' = 33°$ and $\Delta z' = 0.51$, whereas a binary screw axis parallel to *b* would give a value of $\theta' = 30°$, in agreement with the energy calculations.

Structural Refinement. The space groups $P2_12_12_1$ and $P222_1$ were considered in the structural refinement, since they are the only ones that agree with (a) the observed orthorhombic unit cell, (b) the absence of symmetry elements such as inversion centers and mirror or glide planes, which are incompatible with the chiral nature of the polymer, and (c) the symmetry of the molecular chains. In this sense, note that a 2_1 helix with five residues in its asymmetric unit is compatible with the postulated 10_7 conformation.

The $P2_12_12_1$ space group corresponds to a unit cell with two antiparallel molecular chains (Figure 4a) related by 2-fold screw axes parallel to *a* and *b* crystallographic axes. An asymmetric unit made of five consecutive residues was built with the coordinates given by Hoogsteen et al.[5] and the molecular symmetry and was positioned so as to place the center of the resulting helix at *a*/2 and *b*/4 (Figure 4a). In a first step of the refinement process, the setting angle of the asymmetric unit was systematically varied by 5° increments between 0 and −108°, which corresponds to the rotation angle between consecutive residues according to the 10_7 helix conformation. Translations along the *c* axis from 0 to 0.5 (fractional coordinates) with a grid step of 0.05 were also considered for each rotation angle. Note that the explored region is more restricted than that studied in the PCSP calculations due to the imposed space group symmetry. Table 2 gives the fractional coordinates of the first residue in the optimized packing, which corresponds to the variables $\tau = 138°$, $\theta' = 42°$, and $\Delta z' = 0.58$ (or $\theta = -30°$ and $\Delta z = 0.18$, as defined in PCSP calculations). The resulting 0*kl* electron diffraction pattern (Figure 6a) is in close agreement with the experimental one: a *R*-factor lower than 15% was determined by considering the 01*l* and 02*l* reflections. The simulated 0*kl* diffraction patterns are very sensitive to the shift and orientation of chains, and consequently their relative position could be evaluated with precision. Note that the calculated pattern displays a strong 025 reflection, in agreement with experimental evidence, whereas a much weaker reflection is predicted when the packing is modified. This agreement does not hold for the *hk*0 pattern, since violations of systematic absences are observed. Thus, *h*00 and 0*k*0 reflections with *h* and *k* odd appear with a noticeable intensity in our patterns as well as in those previously reported.[11] These violations are not observed in both 0*kl* electron diffraction patterns of epitaxially crystallized samples and X-ray fiber patterns.[5] This suggests that secondary scattering may be responsible for the indicated violations of the axial systematic absences. On the other hand, it is worth noting that the refined packing mode is close to the minimum arrangement labeled as **I** in Figure 5b, i.e. $\theta = -39°$ and $\Delta z = 0.11$, the latter being about 1 kcal/mol more stable than the former. The difference between this minimum-energy packing and that optimized against electron diffraction data is probably due to a deficiency in the PCSP strategy. Indeed, despite its power, the PCSP method has an important shortcoming, namely, that chain conformation is not relaxed for every packing arrangement. Considering fixed chain conformations has important advantages from a computational point of view since the systematic exploration of a large number of packing modes is allowed. Nevertheless, in many cases results must be considered only from a qualitative point of view.[13]

Table 2. Fractional Coordinates of the First Residue Atoms of a Molecular Chain Placed at the Position (0.25, 0.5, *z*) for the Model with a $P2_12_12_1$ Space Group Symmetry and Optimized against 0*kl* Electron Diffraction Data

atom	*x*	*y*	*z*
O	0.348 58	0.619 08	0.001 74
C	0.290 48	0.465 77	0.026 56
O	0.185 32	0.407 46	0.018 72
C	0.375 20	0.378 57	0.065 24
H	0.436 27	0.503 55	0.076 39
C	0.452 05	0.187 12	0.046 88

The $P222_1$ space group is consistent with a statistical arrangement of up and down chains (Figure 4b). Molecules with both orientations and half occupancy can be considered at each site. Note also that no symmetry element relates the molecules that belong to different positions. Thus, four variables (the *z* coordinate and the setting angle for a C^α atom at each site) need be considered. However, this statistical arrangement was not taken into account in the energy analysis because computer packages do not simulate molecules with a half occupancy. No *hk*0 systematic absences are expected for this space group. The intensities found in the simulated patterns for the *h*00 and 0*k*0 reflections (with

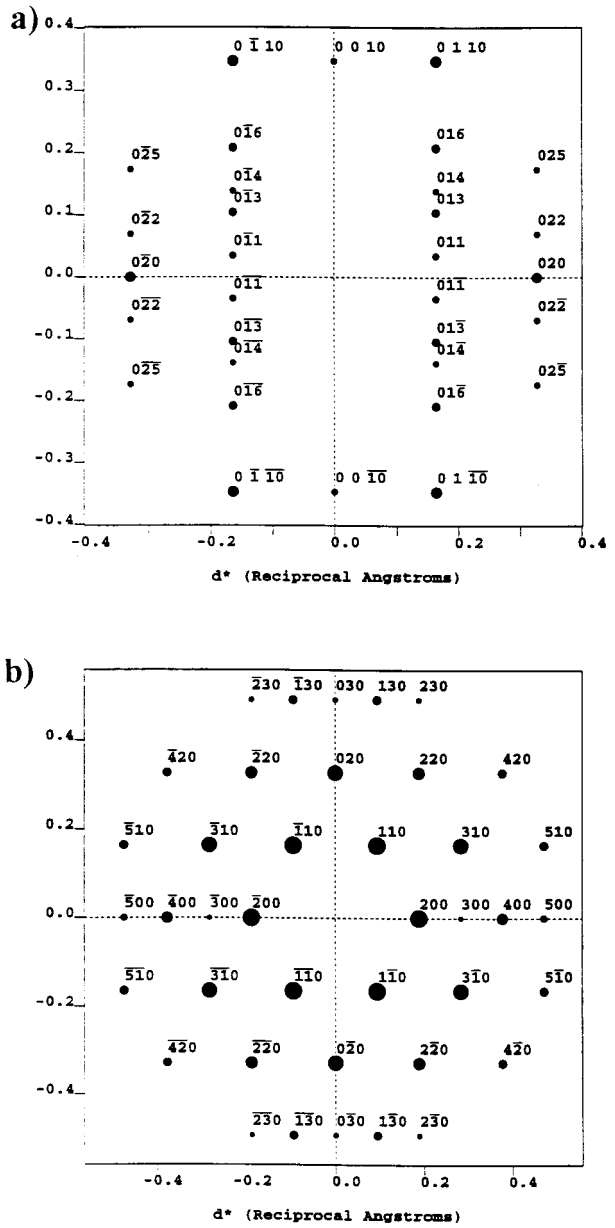

Figure 6. (a) Simulated 0*kl* electron diffraction pattern of the optimized packing of poly(L-lactide) in the $P2_12_12_1$ space group. (b) Simulated *hk*0 electron diffraction pattern of the optimized packing of poly(L-lactide) in the $P222_1$ space group.

h and *k* odd) are far away from the experimental values (Figure 6b). These maximum intensities are observed when the major deviation from the 2-fold screw axis symmetry is reached, that is, for a difference of 18° between the setting angles of molecules at each position. It is worth noting that odd *h*00 or 0*k*0 reflections appear only at high resolution in the simulated patterns. Note also that *hk*0 reflections, with $h + k$ odd, are also only expected at high resolution, and consequently the intense 210 spot is not accounted for. This arises from the fact that chains with a strict 10_7 conformation are very similar in chain axis projection, giving a centered cell at low resolution.

For the sake of completeness the other minimum-energy arrangements obtained from PCSP calculations (Figure 5b) were also considered, although they do not correspond to any orthorhombic space group symmetry. No improvement was reached in the resulting simulated electron diffraction patterns.

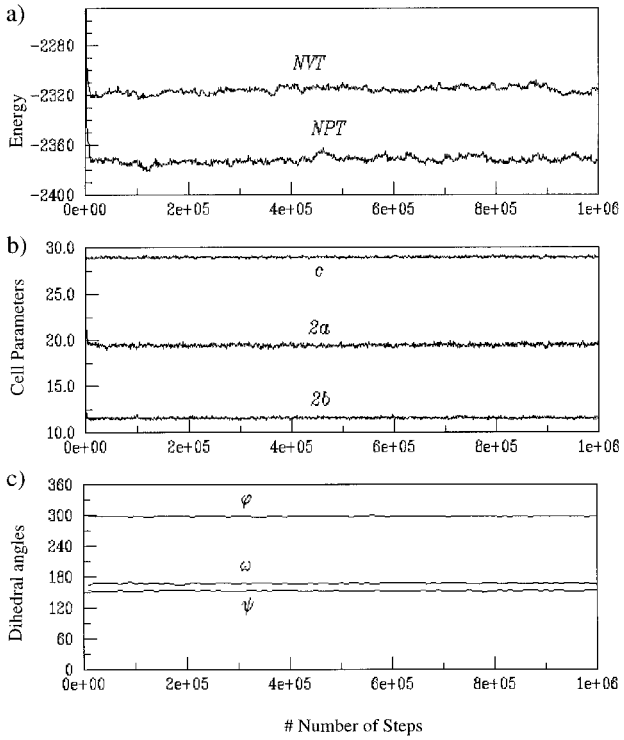

Figure 7. (a) Energy (in kcal/mol) of the system as a function of the number of steps for *NVT* and *NPT* type MC simulations of poly(L-lactide). (b) Cell parameters (in Å) of poly(L-lactide) as a function of the number of steps. (c) Dihedral angles (in deg) of the 10_7 helix as a function of the number of steps for *NPT* type MC simulation of poly(L-lactide).

Monte Carlo Simulations. Two different simulations were performed on the antiparallel arrangement. In both cases the optimized structure with $\tau = 138°$, $\theta = -30°$, and $\Delta z = 0.18$ was used as starting point since it provided the best simulation of the electron diffraction pattern (Figure 6a). The first was of *NVT* type with the torsional angles (φ, ψ, and ω), setting angles (τ and θ) and displacement (Δz) as degrees of freedom. In the second simulation, of *NPT* type, the cell parameters and position of the helices within the simulation box were also varied. Both simulations consist of 1×10^6 steps and were performed at $T = 298$ K.

Figure 7a shows the energy as a function of the number of MC steps for the two simulations. The system equilibrates rapidly, requiring only about 2×10^4 steps. After this, the fluctuations of the energy are small and slightly larger for the *NPT* simulation than for the *NVT* one. In the former indeed, the lattice vibrations induce some changes in the intermolecular forces which are neglected in the simulation at constant volume. Another interesting trend is that the energy resulting from the *NPT* simulation is lower than that of the *NVT* one, since the cell parameters are allowed to vary.

Figure 7b presents the values of the cell parameters *a*, *b*, and *c* obtained from the *NPT* simulation. The three parameters converge to values close to the experimental ones, i.e., $a = 9.66$ Å, $b = 5.80$ Å, and $c = 29.01$ Å (associated errors are 9%, 5%, and 1% for *a*, *b*, and *c*, respectively). This good agreement (in particular for *b* and *c*) indicates that the simulation captures the essential trends of the unit cell, despite a clear systematic deviation: the interchain distances tend to be closer than experimentally measured. A very similar feature was recently found in *NPT* simulations of comblike polyamides.[19] This deviation appears to have a technical

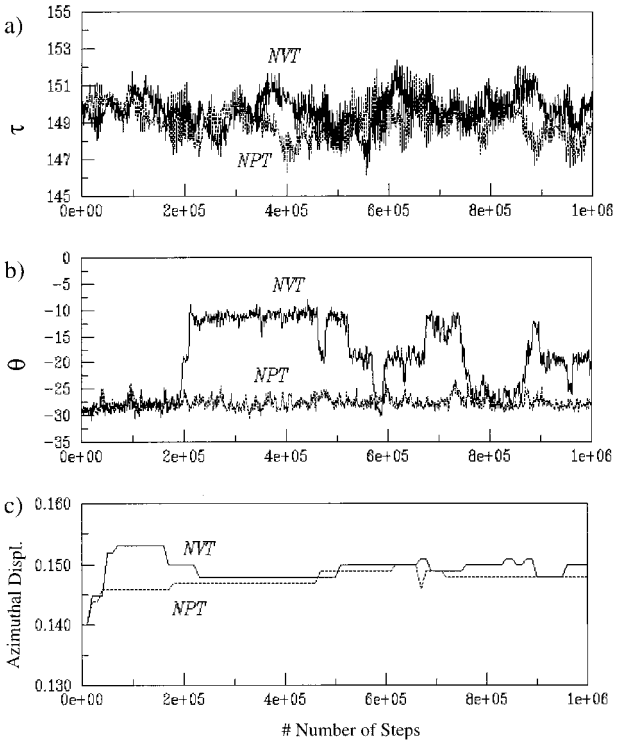

Figure 8. τ (a) and θ (b) setting angles (in deg) as a function of the number of steps for *NVT* and *NPT* type MC simulations of poly(L-lactide). (c) Chain axis shift (in fractional coordinates) as a function of the number of steps for *NVT* and *NPT* type MC simulations of poly(L-lactide).

origen: the parameters included in the AMBER libraries were optimized for the simulation of biological molecules in solution.[14] Poly(L-lactide) is not included in the AMBER libraries, and we have mixed our own electrostatic parameters with the van der Waals parameters of the AMBER force field. Thus, the wave function and the number of points used to develop the electrostatic charges of poly(L-lactide)[15] are different from those used in the original parametrization of the AMBER force field.

The torsional angles resulting from *NVT* and *NPT* simulations are nearly identical, as expected from the small variation of the *c* parameter. Figure 7c shows the torsional angles φ, ψ, and ω as a function of the number of steps for the *NPT* simulation. The final values ($\varphi = -61.4°$, $\psi = 154.2°$, and $\omega = 167.5°$) are close to those proposed by Hoogsteen et al.[5] ($\varphi = -64.8°$, $\psi = 148.9°$, and $\omega = 179.5°$) for the 10_7 helix.

The setting angles τ and θ (and the *c* axis shift Δz) display sharp periodic variations during the *NVT* simulation (Figure 8): changes of about 10°−15° occur when unfavorable interactions appear and the system needs to overcome them. However, when the size of the box is allowed to vary, the system has more degrees of freedom, and the crystal is stabilized by small changes in all of them. As a result, only small variations of τ and θ around 149° and −30°, respectively, are found in the *NPT* simulation, which are very close to the refined values (138° and −30°), whereas the *c* axis shift remains close to the optimized value ($\Delta z \approx 0.18$) in both *NPT* and *NVT* simulations.

Taken in combination, these results indicate that the structural refinement yields a quite stable structure. Furthermore, MC simulations (especially of *NPT* type) help overcome the deficiencies of the PCSP strategy discussed above. Indeed, pilot calculations, i.e., *NPT* simulations of 25×10^4 steps, using as starting point the minimum-energy arrangement labeled as **I** in Figure 5 indicate a spontaneous evolution toward the packing mode refined against electron diffraction data (results not shown). However, the *a* and *b* cell parameters are again underestimated due to the approximations used in the force field.

MC simulations may also account for the chain distortion suggested by the X-ray fiber diffraction data.[5] The near-hexagonal packing (as deduced from the unit cell parameters) of helices with a different symmetry (10_7 conformation) and the antiparallel arrangement are certainly at the root of such distortions. Note that molecular interactions are different in the three packing directions at 120°, which are nearly equivalent. NPT Monte Carlo simulations highlight this feature, since the computed interchain distances indicate a much larger variation along the unit cell diagonal (8.6% for the packing between antiparallel chains) than for the *b* axis (5%), which corresponds to the packing between parallel chains. Furthermore, NVT simulations indicate that unfavorable interactions easily appear when the dimensions of the cell are fixed, giving a variation of the setting angles.

As a final step of the energy analysis, we performed five *NPT* simulations using as starting points the minima obtained form PCSP calculations. These calculations provide a more realistic description of the low-energy packing modes since the shortcomings of the PCSP strategy are avoided. In Table 1, the resulting τ, θ, and Δz parameters and the packing energies are compared with those performed with the PCSP computer program. The MC simulations yield comparable energies and do not help to discriminate the different models. However, the impact of the rigid geometry approximation on the τ, θ, and Δz parameters can be evaluated: the maximum differences found between PCSP and MC arrangements for poly(L-lactide) are 18°, 15°, and 0.07 fractional coordinates, respectively, with the only exception of τ for the minimum **IV**.

Conclusions

Packing energy calculations, structural refinement against electron diffraction data, and Monte Carlo simulations point to the same packing mode, which corresponds to an antiparallel arrangement of molecular chains and a $P2_12_12_1$ space group. Similar setting angles (±6°) and chain axis shift (±0.035) were obtained from the three calculations, which however were based on a strict 10_7 conformation. Several minima with similar energy were also observed in the rather restricted potential energy surface. However, none of these other packing modes are in agreement with diffraction data.

Molecular interactions between neighboring chains are different along the three directions that define the hexagonal packing and may lead to distorted conformations, as revealed by diffraction patterns.

Acknowledgment. This investigation was supported by a research grant from CICYT (MAT2000-0995). J.P. acknowledges financial support from de Departament d'Universitats, Recerca i Societat de la Informacio de la Generalitat de Catalunya. Authors are indebted to the European Center for Parallelism of Barcelona for computational facilities.

References and Notes

(1) Kalb, B.; Pennings, A. J. *Polymer* **1980**, *21*, 607.

(2) Eling, B.; Gogolewski, S.; Pennings, A. J. *Polymer* **1982**, *23*, 1587.
(3) Reeve, M. S.; McCarthy, S. P.; Downey, M. J.; Gross, R. A. *Macromolecules* **1994**, *27*, 825.
(4) Postema, A. R.; Luiten, A. H.; Pennings, A. J. *J. Appl. Polym. Sci.* **1990**, *39*, 1265.
(5) Hoogsteen, W.; Postema, A. R.; Pennings, A. J.; tenBrinke, G.; Zugenmaier, P. *Macromolecules* **1990**, *23*, 634.
(6) Puiggalí, J.; Ikada, Y.; Tsuji, H.; Cartier, L.; Okihara, T.; Lotz, B. *Polymer* **2000**, *41*, 8921.
(7) Cartier, L.; Okihara, T.; Ikada, Y.; Tsuji, H.; Puiggalí, J.; Lotz, B. *Polymer* **2000**, *41*, 8909.
(8) De Santis, P.; Kovacs, J. *Biopolymers* **1968**, *6*, 299.
(9) Arnott, S.; Wonacott, A. J. *J. Mol. Biol.* **1966**, *21*, 371.
(10) Cartier, L.; Okihara, T.; Lotz, B. *Macromolecules* **1997**, *30*, 6313.
(11) Miyata, T.; Masuko, T. *Polymer* **1997**, *38*, 4003.
(12) Kobayashi, J.; Asahi, T.; Ichiki, M.; Okikawa, A.; Suzuki, H.; Watanabe, T.; Fukada, E.; Shikinami, Y. *J. Appl. Phys.* **1995**, *77*, 2957.
(13) León, S.; Navas, J. J.; Alemán, C. *Polymer* **1999**, *40*, 7351.
(14) Weiner, S. J.; Kollan, P. A.; Nguyen, D. T.; Case, D. A. *J. Comput. Chem.* **1986**, *7*, 230.
(15) Alemán, C.; Luque, F. J.; Orozco, M. *J. Comput.-Aided Mol. Des.* **1993**, *7*, 721.
(16) Cerius^2 1.6, Molecular Simulations Inc., Burlington, MA.
(17) León, S.; Alemán, C.; Escalè, F.; Laso, M. *J. Comput. Chem.* **2001**, *22*, 162.
(18) Metropolis, N.; Rosenbluth, A. W.; Rosenbluth, M. N.; Teller, A. H.; Teller, E. *J. Chem. Phys.* **1953**, *21*, 1087.
(19) León, S.; Alemán, C.; Muñoz-Guerra, S.; Laso, M. *J. Theor. Comput. Polym. Sci.* **2000**, *10*, 177.

MA001630O